

## Geometry effects on Rayleigh-Bénard convection in rotating annular layers

J. J. Sánchez-Álvarez,<sup>1</sup> E. Serre,<sup>2</sup> E. Crespo del Arco,<sup>3</sup> and F. H. Busse<sup>4</sup>

<sup>1</sup>*E.T.S.I. Aeronáuticos, Universidad Politécnica de Madrid, Madrid 28040, Spain*

<sup>2</sup>*M2P2 UMR7340 CNRS, Aix-Marseille Université, Ecole Centrale Marseille, Technopôle de Château-Gombert, 13451 Marseille, France*

<sup>3</sup>*U.N.E.D., Departamento Física Fundamental, Apartado 60.141, 28080 Madrid, Spain*

<sup>4</sup>*Institute of Physics, University of Bayreuth, D-95440 Bayreuth, Germany*

(Received 25 November 2013; published 23 June 2014)

Rayleigh-Bénard convection is investigated in rotating annular cavities at a moderate dimensionless rotation rate  $\Omega = 60$ . The onset of convection is in the form of azimuthal traveling waves that set in at the sidewalls and at values of the Rayleigh number significantly below the value of the onset of convection in an infinitely extended layer. The present study addresses the effects of curvature and confinement on the onset of sidewall convection by using three-dimensional spectral solutions of the Oberbeck-Boussinesq equations. Such solutions demonstrate that the curvature of the outer boundary promotes the onset of the wall mode, while the opposite curvature of the inner boundary tends to delay the onset of the wall mode. An inner sidewall with a radius as low as one tenth of its height is sufficient, however, to support the onset of a sidewall mode. When radial confinement is increased the two independent traveling waves interact and eventually merge to form a nearly steady pattern of convection.

DOI: [10.1103/PhysRevE.89.063013](https://doi.org/10.1103/PhysRevE.89.063013)

PACS number(s): 47.54.-r

### I. INTRODUCTION

Flows induced by thermal buoyancy in rotating systems play an important role in many industrial processes as well as in numerous problems of geophysical and astrophysical fluid dynamics. For this reason numerous theoretical investigations and laboratory experiments have been devoted to the properties of convection in rotating layers. A peculiar property is the subject of this paper, namely the fact that the onset of convection may occur first at the sidewall of the fluid layer.

For a laterally unbounded horizontal layer with constant temperatures  $T_1$  and  $T_2$ ,  $T_1 > T_2$ , applied at bottom and top, respectively, and rotating about a vertical axis it has been established by Chandrasekhar that overstability is only possible if the Prandtl number is below a certain value of about 0.69 [1]. Here the Prandtl number denotes the ratio between the kinematic viscosity  $\nu$  and the thermal diffusivity  $\kappa$ . When a rotating fluid layer is bounded by lateral rigid sidewalls, however, the onset of convection can occur via a supercritical Hopf bifurcation for all Prandtl numbers [2]. When the Coriolis number, which is defined by  $\Omega = 2\pi f d^2/\nu$ , where  $f$  is the rotation frequency and  $d$  is the height of the layer, is greater than about 30 [3], the onset of sidewall modes becomes preferred in comparison with the onset of convection in the bulk and the instability of the state of pure conduction occurs via a traveling wave attached to the sidewall. As expected for a supercritical bifurcation, the amplitude of the sidewall convection grows in proportion to  $\sqrt{\text{Ra} - \text{Ra}_c}$ . Here the definition  $\text{Ra} = g\alpha d^3(T_1 - T_2)/\nu\kappa$  is used for the Rayleigh number, with gravity  $g$  and coefficient of thermal expansion  $\alpha$ . The onset of the traveling wave attached to the sidewall is facilitated by the fact that part of the Coriolis force is balanced by the pressure.

The so-called wall mode has been widely studied experimentally and theoretically in the past years mainly within cylindrical cavities. It was first experimentally identified through shadowgraph imaging in 1991 [4]. The critical

Rayleigh number for the onset of the wall mode has been determined numerically in Ref. [5]. At small amplitudes its dynamics is well described by a complex Ginzburg-Landau equation (CGL) [6]. The coefficients of the CGL equation have been determined experimentally [6] and numerically [7] with good agreement. In Ref. [7] the onset of the wall mode in a cylinder of aspect ratio  $\Gamma = 1$  has been studied numerically. Here  $\Gamma$  denotes the ratio of radius to height of the cylindrical box. Also the limit cases of  $\Omega \rightarrow \infty$  [8] or of a very narrow channel [9] have been studied.

In this study, we are concerned with rotating Rayleigh-Bénard convection in an annular gap between two coaxial cylindrical boundaries. Such a system allows us to investigate linear and nonlinear properties of waves at the inner and the outer boundary of the annular layer. In comparison with convection in a rotating cylinder, the convection planform is strongly dependent on the two geometric parameters which are the radii ratio and the aspect ratio. Most theoretical analyses of wall-attached convection assume the idealization of planar sidewalls. Liao *et al.* [10] have performed linear and weakly nonlinear analysis of the case of rapidly rotating straight channels to study the dependence of the convection planform on the aspect ratio and on the Prandtl number. When curvature becomes significant, the two oppositely traveling modes are characterized by different critical Rayleigh numbers and complex Ginzburg-Landau equations are no longer applicable. Three-dimensional numerical simulations of fully nonlinear convection have been reported by Li *et al.* [11], who focused their study on the interactions between the inner and outer wall modes. These nonlinear simulations revealed interesting new solutions when the two oppositely traveling three-dimensional waves interfere intensively.

The present study is primarily concerned with the effect of the curvature on the onset of wall modes convection at a moderate rotation rate,  $\Omega = 60$ , which is typical for the regime between the minimum value of  $\Omega$  for the onset of the sidewall mode and the high value of  $\Omega = 500$  used by Li *et al.* [11].

The asymptotic theory of Ref. [11] suggests that the results presented in the present paper are qualitatively correct at even higher values of  $\Omega$ . The characteristic length scales decrease with increasing  $\Omega$  and the numerical effort required for their resolution will have to increase. The chosen value of  $\Omega$  thus appears to be an optimal one.

We are interested in the onset of convection in finite annular channels in which the dynamical asymmetry of the modes at the inner and outer curved walls becomes important. When the channel width is sufficiently large with respect to the radial extension of wall modes, the nonlinear interaction of the waves near the onset is weak such that they can be studied independently on both concave and convex walls. On the other hand, when the channel is narrow, the two oppositely traveling three-dimensional waves always interact nonlinearly.

The paper starts with the mathematical formulation of the problem and an outline of the numerical method for direct numerical simulations in Sec. II. Results of the numerical study are presented in Secs. III and IV. We first present the curvature dependence of the convection onset in annular cavities with moderate to high curvatures of the inner sidewall (small to moderate radii ratio), then turn to the radial confinement effect for annular cavities with aspect ratios of the order unity. An outlook on convection at higher Rayleigh numbers is given in Sec. V.

## II. NUMERICAL INTEGRATION OF THE BOUSSINESQ EQUATIONS

We are considering a horizontal annular fluid layer heated from below of height  $d$  with outer radius  $r_{\text{out}} = d\Gamma_{\text{out}}$  and inner radius  $r_{\text{in}} = d\Gamma_{\text{in}}$  (Fig. 1). Such a geometry is fully characterized by its aspect ratio  $L \equiv \Gamma_{\text{out}} - \Gamma_{\text{in}}$  and its radii ratio  $\chi \equiv \Gamma_{\text{in}}/\Gamma_{\text{out}}$ .

As in most works on convection in rotating layers we adopt the Oberbeck-Boussinesq approximation in that the temperature dependence of the density is taken into account only in the gravity term. The temperature difference applied between the lower and upper boundary is  $T_1 - T_2$ . The temperature is made dimensionless using the definition  $T = [T^* - (T_2 + T_1)/2]/(T_1 - T_2)$ , where  $T^*$  represents the dimensional temperature. Using  $d$ ,  $d^2/\kappa$ , and  $\kappa/d$  as scales for length, time, and velocity, respectively, we write the equations of motion relative to the rotating frame of reference and the

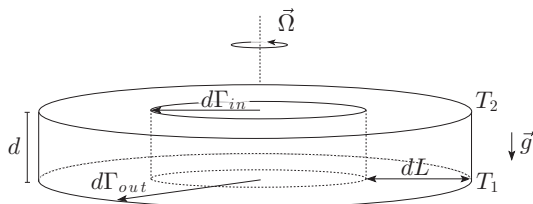


FIG. 1. Geometrical model of the problem of Rayleigh-Bénard convection in an rotating annular cavity with height  $d$ , inner radius  $r_{\text{in}} = d\Gamma_{\text{in}}$ , outer radius  $r_{\text{out}} = d\Gamma_{\text{out}}$ , and aspect ratio  $L = \Gamma_{\text{out}} - \Gamma_{\text{in}}$ . The lower and upper boundaries are kept at constant temperatures  $T_1$  and  $T_2$ , respectively, being  $T_1 > T_2$ .

heat equation as follows:

$$\frac{1}{\text{Pr}} \left( \frac{\partial \mathbf{V}}{\partial t} + \mathbf{V} \cdot \nabla \mathbf{V} \right) = -\nabla p - 2\Omega \hat{\mathbf{z}} \times \mathbf{V} + \nabla^2 \mathbf{V} + \text{Ra} T \hat{\mathbf{z}}, \quad (1)$$

$$\nabla \cdot \mathbf{V} = 0, \quad (2)$$

$$\frac{\partial T}{\partial t} + \mathbf{V} \cdot \nabla T = \nabla^2 T, \quad (3)$$

where  $\Omega$ ,  $\text{Pr}$ , and  $\text{Ra}$  are the Coriolis, Prandtl, and Rayleigh numbers, respectively, defined in the introduction.  $\hat{\mathbf{z}}$  is the unit vector in the axial direction (opposite to the direction of gravity). For an annular channel it is convenient to introduce a cylindrical polar coordinate system  $(r, \theta, z)$ . The velocity components are  $\mathbf{V} = (V_r, V_\theta, V_z)$  and  $p$  is the dynamic pressure. In order to focus the attention on the sidewall mode we assume that the centrifugal force is negligible,  $r_{\text{out}}\Omega^2 \ll gd^4/\nu^2$ , which is quite well approached in most experiments [4]. For a recent analysis of the wall mode in the presence of the centrifugal force, see Ref. [12].

Highly conducting upper and lower boundaries are assumed such that the temperature  $T$  is fixed at the values  $T = \mp 0.5$  at  $z = \pm 0.5$ . No-slip boundary conditions ( $V_r = V_\theta = V_z = 0$ ) are applied at all walls since these are fixed in the rotating frame. Insulating thermal boundary conditions are used at the vertical sidewalls since this kind of boundary condition is most relevant to experiments in which Plexiglas is often used.

Numerical solutions of Eqs. (1)–(3) are obtained through a pseudospectral collocation–Chebyshev expansion in both the radial and the axial directions  $(r, z)$ , and a Fourier expansion is used in the azimuthal direction. This choice takes into account the orthogonality properties of Chebyshev polynomials and, in particular, provides exponential convergence, referred to as spectral accuracy [13]. The time integration scheme is semi-implicit second-order accurate. It corresponds to a combination of the second-order Euler backward differentiation formula and the Adams-Bashforth scheme for the nonlinear terms. The capability and the accuracy of the present code to model various rotating Rayleigh-Bénard phenomena have already been exemplified in Refs. [14,15]. A single grid with mesh  $(33 \times 128 \times 33)$  in the radial, azimuthal, and axial directions has been used. Such mesh is reliable because the dependence of the solution on both the vertical and the radial coordinates remains smooth. In particular at the moderate rotation rate  $\Omega = 60$ , the Ekman layers at the top and bottom boundaries are well resolved with a minimum of four mesh points in each boundary layer because of the decreasing mesh size due to the Gauss-Lobatto points distribution near the boundary. For all parameters, spectral coefficients series of any solution have been shown to converge.

The corresponding time step is equal to  $\delta t = 5 \times 10^{-3}$ . Computations are initialized from a conducting state corresponding to a fluid at rest. When the Rayleigh number is increased the linear profile of the temperature is perturbed by a white noise with an amplitude of 0.1%.

The HPC resources of CNRS at IDRIS have allowed us to perform three-dimensional numerical simulations of time-dependent solutions over a wide range of geometrical parameters.

**III. CURVATURE DEPENDENCE OF ONSET OF CONVECTION ON SIDEWALLS**

As mentioned in Sec. II the annular channel is fully characterized by its aspect ratio  $L$  and its radii ratio  $\chi$ . These two parameters define the relative channel width and the relative sidewall curvatures, respectively. Curvature is defined from a combination of these two parameters. When confinement is not too strong and curvature effect is physically significant, stability analysis of a rotating annulus by Li *et al.* [11] reveals that convective instability at the onset assumes the form of a single retrogradely propagating wave attached to the outer sidewall. When the radius ratio  $\chi$  is moderate, meaning that curvatures of both sidewalls are of the same order of magnitude, convection slightly above the onset gives rise to another progradely propagating wave attached to the inner sidewall. The frequencies, wave numbers, and critical Rayleigh numbers of these two oppositely traveling waves are different, leading eventually to nonlinear interactions as investigated by Li *et al.* [11].

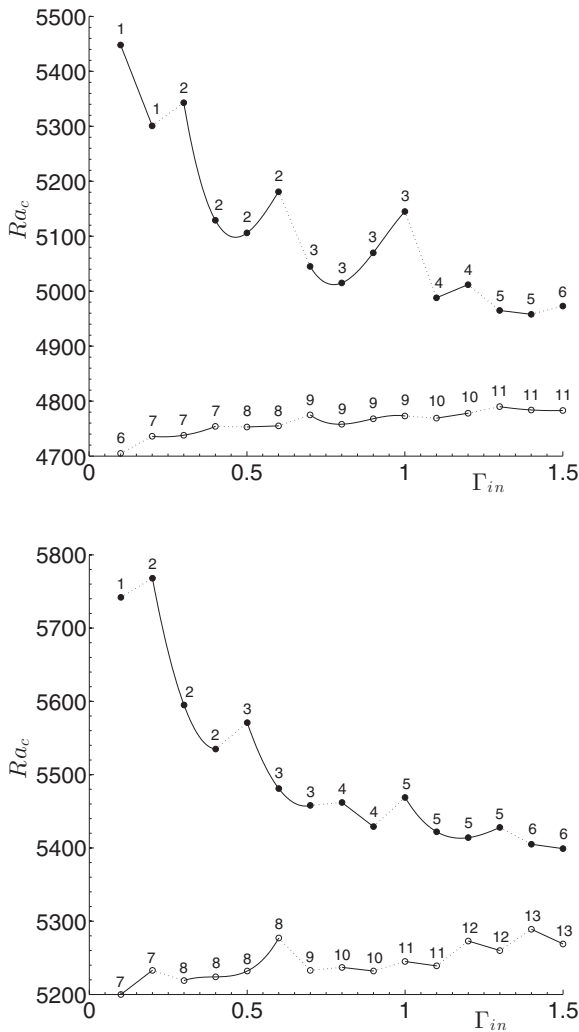


FIG. 2. Critical Rayleigh number,  $Ra_c$ , at the inner sidewall region (closed circles) and at the outer sidewall region (open circles), vs dimensionless inner radius,  $\Gamma_{in}$ , for  $Pr = 0.7$  (top) and  $Pr = 5.3$  (bottom). The numbers above the data points indicate azimuthal wave number of the selected mode. The lines are only a guide to the eye.

In this section, we are interested in the effects of the curvature on the onset of sidewall convection along the convex inner and the concave outer wall. When the annular region is sufficiently wide, the onsets of convection at the inner and the outer sidewalls occur nearly independently and the interaction of the two modes is negligible at values of  $Ra$  close to onset.

Nonlinear computations have been carried out in a cavity with a fixed aspect ratio  $L = 2$ . That corresponds to a good compromise between weak confinement and computational savings since a rough estimate of the radial extension of wall modes yields about 0.2 in dimensionless units at moderate rotation rate  $\Omega = 60$ , according to the asymptotic analysis of Hermann and Busse [8] for a plane wall. Curvature is varied by changing the cavity in a range of dimensionless inner radii,  $0.1 \leq \Gamma_{in} \leq 1.5$ , that corresponds to a variation of the curvature parameter  $\chi$  in the range  $0.048 \leq \chi \leq 0.43$ . Since all computations have been for the fully nonlinear system of Eqs. (1)–(3), the critical values of Rayleigh number  $Ra_c$  are determined by using the property that the kinetic energy of convection increases linearly with  $Ra$  for a limited region above  $Ra_c$ . The azimuthally averaged square of the vertical velocity at the distance of 0.12 from the sidewalls on the midplane of the layer is computed at several supercritical Rayleigh numbers. Those values exhibit a well-defined linear dependence on  $Ra$  that can reliably be extrapolated to zero for the determination of the critical values  $Ra_c$  for the onset of sidewall convection at the inner as well as the outer sidewall. Results for the inner and the outer sidewalls are shown in Fig. 2 for two different Prandtl numbers.

For the convection at the inner wall, critical value of the Rayleigh numbers  $Ra_c$  show the expected trend predicted by linear stability analysis [11], namely that they increase with decreasing the inner radius. In other words, curvature inhibits sidewall convection at the inner wall. But even when the curvature is very strong, corresponding to a very small inner radius, typically  $r_{in} = 0.1d$  here, it cannot prevent the onset of sidewall convection. Contrary to what one might have expected, solutions show that sidewall convection can occur on an inner sidewall having a perimeter much smaller than the theoretical azimuthal wavelength, which is about  $2.1d$  [5]. This is evident from the  $m = 1$  wave shown in Fig. 3 in the case of an inner radius  $r_{in} = 0.1d$ . Our numerical simulations show the opposite trend for convection on the outer sidewall with a destabilization effect of the curvature. The critical Rayleigh

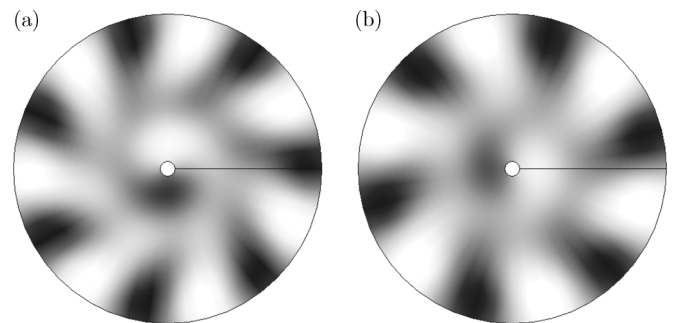


FIG. 3. Isotherms at midheight in an annular cavity with  $\Gamma_{in} = 0.1$  and  $L = 2$  at  $\Omega = 60$ . (a)  $Pr = 5.3$ ,  $Ra = 6150$ . (b)  $Pr = 0.7$ ,  $Ra = 5750$ .

number may appear to be less sensitive to curvature on this sidewall but it is simply because the curvature variations between two outer radius positions are smaller than on the inner sidewall.

In the limit of large inner radii, critical Rayleigh numbers on both sidewalls seems to tend to a single asymptotic value that is about  $Ra_c = 4900$  and  $Ra_c = 5300$  for  $Pr = 0.7$  and  $Pr = 5.3$ , respectively. These values agree reasonably well with the critical Rayleigh numbers for a straight channel obtained in Ref. [8]. Please note a misprint in the caption of Fig. 2 of the latter paper: It should be  $\tau^2 = 4\Omega^2 d^4 / \nu^2$ .

A property of the plots in Fig. 2 is that the values of  $Ra_c$  do not vary monotonically. That is caused by the discrete nature of the azimuthal wave numbers  $m$ . Since the minimizing value of  $m$  stays constant for a certain range of sidewall curvature, this value of  $m$  is no longer quite optimal at the ends of this range where it competes with values  $m + 1$  or  $m - 1$ .

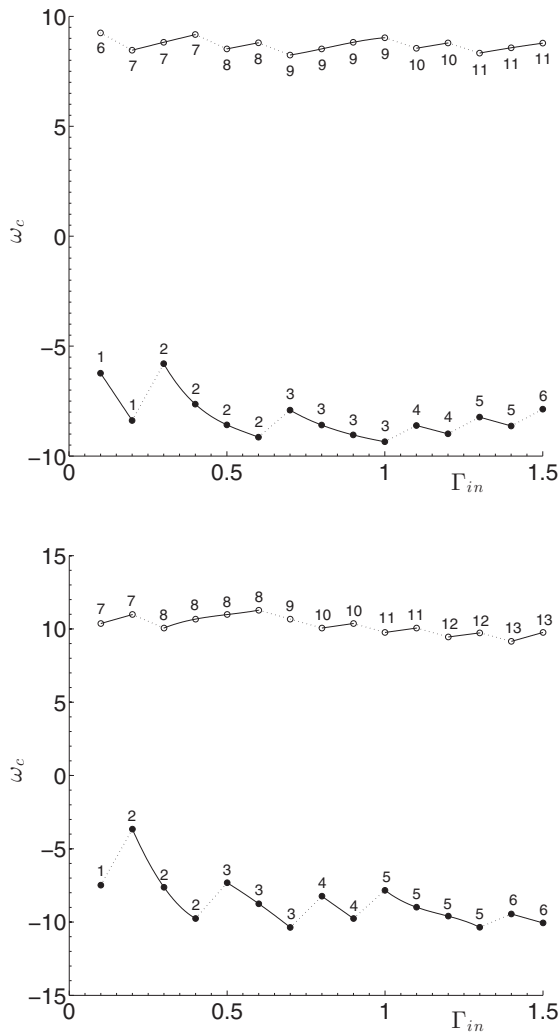


FIG. 4. Critical frequency,  $\omega_c$ , for the inner sidewall mode (closed circles) and for the outer sidewall mode (open circles), vs dimensionless inner radius,  $\Gamma_{in}$ , for  $Pr = 0.7$  (top) and  $Pr = 5.3$  (bottom). The numbers over the circles indicates azimuthal wave numbers of the nonlinearly selected mode. The lines are only a guide to the eye.

The frequency exhibits a linear dependence with  $Ra - Ra_c$ , with a finite intercept at onset [16]. This behavior allow us to compute the critical frequencies at onset. The results are shown in Fig. 4 for two different Prandtl numbers.

#### IV. INTERACTIONS OF SIDEWALL CONVECTION IN ANNULAR LAYERS

In this section, we are interested in the confinement effect on the onset of sidewall convection. We consider three rotating annular cavities with aspect ratios  $L$  less than the dimensionless inner radius  $\Gamma_{in}$  which is kept constant,  $\Gamma_{in} = 7.5$ , in all three cases. The aspect ratio  $L$  is lowered from  $L = 5$  to  $L = 1.5$  and  $L = 0.75$  in order to increase the confinement. In contrast to the previous section, the radius ratios are varying from  $\chi = 0.6$ ,  $\chi = 0.75$ , to  $\chi = 0.9$  in the three cases. For this range of  $\chi$ , the curvatures of both sidewalls are close in absolute value and two oppositely traveling waves can be expected near the onset of convection. Their nonlinear interactions has previously been observed by Li *et al.* [11] at  $\chi = 0.75$  for  $\Omega = 300$ . Since the critical Rayleigh number for sidewall convection is given by about  $Ra_c = 5340$ , we are carrying out our computations at  $Ra = 5600$  which is about 5% above the onset.

For  $L = 5$ , the annular channel is sufficiently wide and the two sidewall modes do not interact and travel in opposite directions as shown in Fig. 5(a) while the fluid in the interior between the walls is nearly at rest. Both waves have nearly the same absolute values of their frequencies and wave numbers,  $\omega_{in} = -9.87$ ,  $\omega_{out} = +9.99$ , and  $k_{in} = 4.13$ ,  $k_{out} = 4.08$ , respectively.

For  $L = 1.5$ , the annular channel is sufficiently narrow now such that some interaction between the oppositely traveling waves occurs as it is apparent in Fig. 5(b). The inner and outer travelling waves are characterized by their wave numbers  $k_{in} = 3.73$ ,  $k_{out} = 3.66$  and the corresponding frequencies  $\omega_{in} = -10.09$ ,  $\omega_{out} = +9.08$ . This interaction occurs in the form of a nearly linear superposition as is shown in Fig. 6, where the  $z$  velocity in the middle of the channel at midheight has been plotted as a function of time. This temporal signal exhibits a period of 6.09, which corresponds to the sum  $\omega_b = \omega_{out} + \omega_{in} = +1.01$  of the traveling wave frequencies. In this intermediate region a pairing between the convection

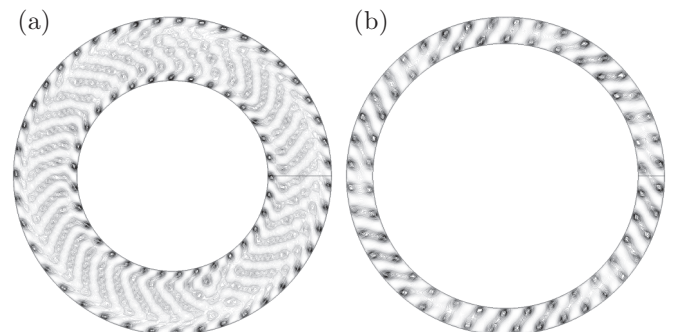


FIG. 5. Isotherms at midheight in an annular cavity with  $\Gamma_{in} = 7.5$  for  $Pr = 5.3$  at  $\Omega = 60$ . (a) Sidewall traveling waves ( $L = 5$ ,  $Ra = 5600$ ). (b) Interaction of two counter-rotating waves in a narrow annular cavity ( $L = 1.5$ ,  $Ra = 5600$ ).

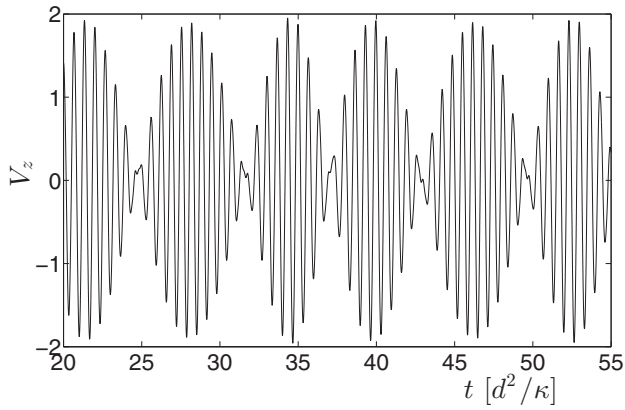


FIG. 6. Vertical velocity at the middle of the cross section of the annular channel as function of time for the same parameter values as in Fig. 5(b).

structures on opposite sides of the annular layer can be observed leading to transverse rolls. Owing to the opposite drifts of the sidewall modes the rolls get stretched in the direction parallel to the sidewalls until they break and new transverse rolls are formed. A similar situation at much higher rotation is shown in Ref. [11].

For  $L = 0.75$ , the width of the channel is of the same order of magnitude as the radial extent of the sidewall modes, and the latter can no longer be realized as separate waves. Instead they combine to form a nearly steady pattern of convection in the form of rolls oriented nearly perpendicular to the sidewalls as shown in Fig. 7. In the limit of an infinite radius corresponding to a straight channel both sidewalls are equivalent and a steady

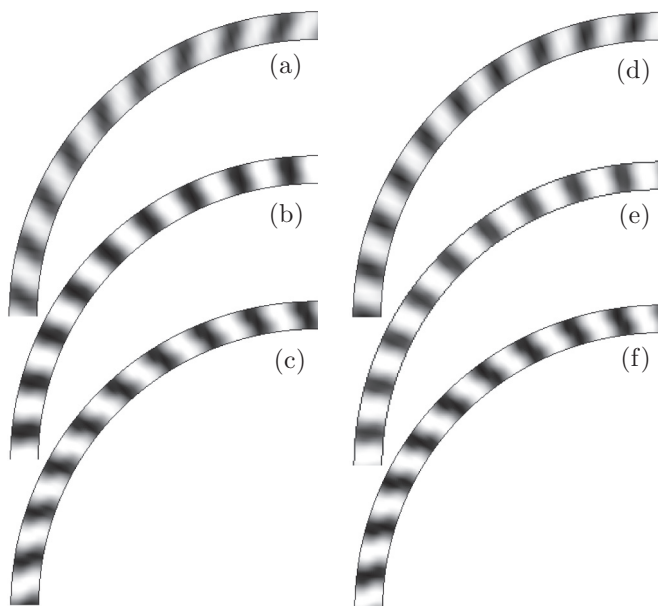


FIG. 7. Convection patterns in the narrow channel with  $L = 0.75$ ,  $\Gamma_{in} = 7.5$ , for  $\Omega = 60$ . (left)  $Pr = 5.3$  and (a)  $Ra = 6000$ , (b)  $Ra = 12000$ , and (c)  $Ra = 17600$ . (right)  $Pr = 0.7$  and (d)  $Ra = 6000$ , (e)  $Ra = 8000$ , and (f)  $Ra = 12000$ . Only a quarter of the cavity is shown (view from the top).

convection pattern must be expected [9,10,17]. In the present configuration the dominance of the mode at the outer wall gives rise to a pattern drifting steadily in the retrograde direction with a frequency somewhat larger than the sum of the two sidewall mode frequencies. The orientation of the rolls is not strictly radial but exhibits a spirallike inclination turning inward in the prograde direction, at least for lower values of  $Ra$ .

When increasing Rayleigh number, the direction of spiralling changes sign ( $Ra = 12000$ ) and at high Rayleigh numbers ( $Ra = 17600$ ) the angle reflects a spiral turning outward with the sense of rotation (see Fig. 7). This change can be attributed to an increasing mean shear in the channel. The steady convection is associated with a mean axisymmetric azimuthal flow. In the limit of an infinite radius of the channel the flow will be antisymmetric with respect to the vertical midplane of the channel. Near the upper and lower boundaries there are slight reversals of this shear flow which can also be seen, for instance, in the related problem treated by Plaut [7]. The average over the height of channel of this flow is shown in Fig. 8 and it is evident that its amplitude

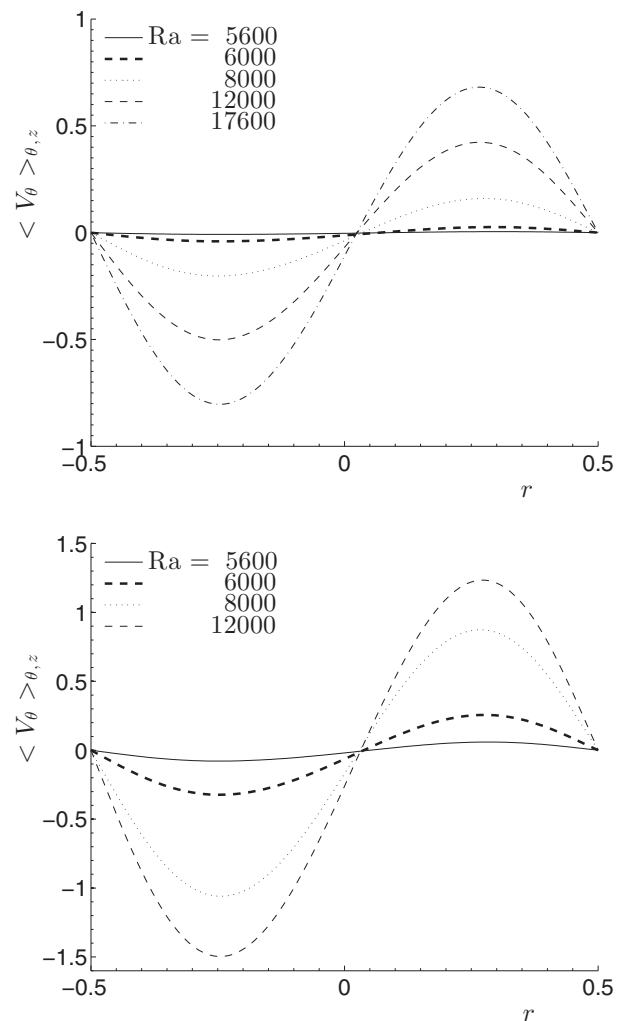


FIG. 8. Vertically averaged profiles of the axisymmetric component of the azimuthal velocity  $V_\theta$  for  $Pr = 5.3$  (top) and  $Pr = 5.3$  (bottom) for the cases of Fig. 7.

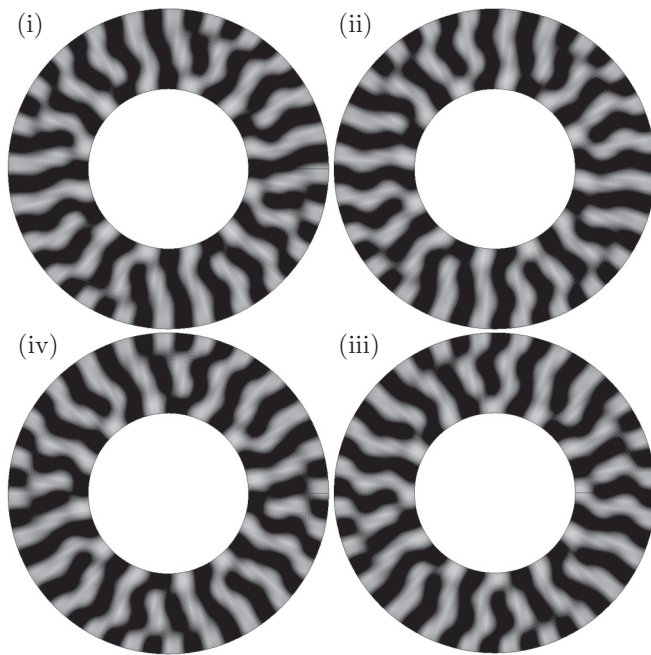


FIG. 9. Temporal evolution of a very nearly periodic pattern for  $\Gamma_{\text{in}} = 3$ ,  $L = 3$ ,  $\Omega = 60$ ,  $\text{Pr} = 5.3$ ,  $\text{Ra} = 7000$ . The pattern is shown at four subsequent time steps separated by the time  $1.75 \times 10^{-2}[d^2/\kappa]$ . The sense of time is followed clockwise such that a fifth plot would be nearly identical to plot (i).

increases strongly with the Rayleigh number. At  $\text{Ra} = 17\,600$  in the case of  $\text{Pr} = 5.3$  and at  $\text{Ra} = 12\,000$  in the case of  $\text{Pr} = 0.7$  the amplitude of the mean shear has become strong enough to clearly reverse the sense of spiraling of the convection rolls. The Prandtl number dependence of this effect is easily understood by looking at Eq. (1), according to which the Reynolds stress term is multiplied by  $\text{Pr}^{-1}$ .

## V. OUTLOOK ON CONVECTION AT HIGHER RAYLEIGH NUMBER

The dynamics of the sidewall modes of convection which has been the subject of this paper is only a particularly simple part of the dynamics of convection in rotating annular layers. Rather chaotic pattern evolutions may be observed at higher Rayleigh numbers than those considered in this paper. Besides the two sidewall convection waves propagating in opposite azimuthal directions, interior convection rolls can be observed when the aspect ratio  $L$  is sufficiently large, say,  $L > 2.5$ . Besides their interaction with the sidewall modes, the interior convection is influenced by the dynamics of the Küppers-Lortz instability [18]; for an experimental realisation see Ref. [19].

Here we give an impression of such a time-dependent state of convection by the example shown in Fig. 9. A particularly simple case has been chosen by ensuring that the wave numbers  $m_{\text{in}}$  and  $m_{\text{out}}$  of the sidewall modes satisfy the ratio 2,  $m_{\text{in}} = 12$  and  $m_{\text{out}} = 24$ . Thus the pattern in each of the four pictures of Fig. 9 exhibits a fourfold periodicity in azimuth. Even with this symmetry and even when a shift in azimuth is allowed for, the pattern is not strictly periodic in time, however.

Highly chaotic patterns are seen when the Rayleigh number and the aspect ratio  $L$  are increased in the absence of simple ratios  $m_{\text{out}}/m_{\text{in}}$ . The incessantly propagating sidewall modes, however, provide a regularity to this convection chaos, the beauty of which can be captured only in a movie.

## ACKNOWLEDGMENTS

This research was partially supported by the Spanish Ministry of Education, under Grants No. TRA2010-18054 and No. FIS2011-24642. F.H.B. acknowledges the support of this research by NASA Grant No. NNX-09AJ85G. The authors were granted access to the HPC resources of IDRIS under the allocations 2013-0242 by GENCI.

- 
- [1] S. Chandrasekhar, *Hydrodynamic and Hydromagnetic Stability* (Dover, New York, 1961).
  - [2] R. E. Ecke, F. Zhong, and E. Knobloch, *Europhys. Lett.* **19**, 177 (1992).
  - [3] E. Y. Kuo and M. C. Cross, *Phys. Rev. E* **47**, R2245 (1993).
  - [4] F. Zhong, R. Ecke, and V. Steinberg, *Phys. Rev. Lett.* **67**, 2473 (1991).
  - [5] H. F. Goldstein, E. Knobloch, I. Mercader, and M. Net, *J. Fluid Mech.* **248**, 583 (1993).
  - [6] Y. Liu and R. E. Ecke, *Phys. Rev. Lett.* **78**, 4391 (1997).
  - [7] E. Plaut, *Phys. Rev. E* **67**, 046303 (2003).
  - [8] J. Herrmann and F. H. Busse, *J. Fluid Mech.* **255**, 183 (1993).
  - [9] F. H. Busse, *J. Fluid Mech.* **537**, 145 (2005).
  - [10] X. Liao, K. Zhang, and Y. Chang, *Geophys. Astrophys. Fluid Dyn.* **99**, 445 (2005).
  - [11] L. Li, X. Liao, K. H. Chan, and K. Zhang, *Phys. Rev. E* **78**, 056303 (2008).
  - [12] J. Curbelo, J. M. Lopez, A. M. Mancho, and F. Marques, *Phys. Rev. E* **89**, 013019 (2014).
  - [13] E. Serre and J. P. Pulicani, *Comp. Fluids* **30**, 491 (2001).
  - [14] E. Serre, E. Crespo del Arco, and F. H. Busse, in *Nonlinear Dynamics in Fluids*, edited by F. Marqués and A. Meseguer (CIMNE, Barcelona, 2003).
  - [15] J. J. Sánchez-Álvarez, E. Serre, E. Crespo del Arco, and F. H. Busse, in *Chaos, Complexity, and Transport: Theory and Applications* (World Scientific, Singapore, 2007), pp. 207–216.
  - [16] F. Zhong, R. Ecke, and V. Steinberg, *J. Fluid Mech.* **249**, 135 (1993).
  - [17] K. Zhang, X. Liao, X. Zhan, and R. Zhu, *Phys. Fluids* **18**, 124102 (2006).
  - [18] G. Küppers and D. Lortz, *J. Fluid Mech.* **35**, 609 (1969).
  - [19] F. H. Busse and K. E. Heikes, *Science* **208**, 173 (1980).